Available online at www.sciencedirect.com
ScienceDirect
Journal of Nuclear Materials 357 (2006) 19–30
journal of nuclear materials
www.elsevier.com/locate/jnucmat

# A computationally simple model for determining the time dependent spectral neutron flux in a nuclear reactor core

E.A. Schneider [a], M.R. Deinert [b,*], K.B. Cady [b]

[a] Department of Mechanical Engineering, University of Texas, Austin, TX, United States
[b] Theoretical and Applied Mechanics, Cornell University, 219 Kimball Hall, Ithaca, NY 14853, United States

Received 5 December 2005; accepted 10 April 2006

**Abstract**

The balance of isotopes in a nuclear reactor core is key to understanding the overall performance of a given fuel cycle. This balance is in turn most strongly affected by the time and energy-dependent neutron flux. While many large and involved computer packages exist for determining this spectrum, a simplified approach amenable to rapid computation is missing from the literature. We present such a model, which accepts as inputs the fuel element/moderator geometry and composition, reactor geometry, fuel residence time and target burnup and we compare it to OECD/NEA benchmarks for homogeneous MOX and UOX LWR cores. Collision probability approximations to the neutron transport equation are used to decouple the spatial and energy variables. The lethargy dependent neutron flux, governed by coupled integral equations for the fuel and moderator/coolant regions is treated by multigroup thermalization methods, and the transport of neutrons through space is modeled by fuel to moderator transport and escape probabilities. Reactivity control is achieved through use of a burnable poison or adjustable control medium. The model calculates the buildup of 24 actinides, as well as fission products, along with the lethargy dependent neutron flux and the results of several simulations are compared with benchmarked standards.


## 1. Introduction

Determining the time dependent balance of isotopes in a nuclear reactor is of central importance in modeling nuclear fuel cycles. The evolving composition of reactor fuel during burnup affects its reactivity, material and chemical properties, as well as the radiative environment to which structural and cladding elements are subjected. In addition, spent fuel isotopic composition is the dominant factor determining the radiation field and head load under which storage and disposal materials must operate. Because of this, computing the isotopic flows through a reactor is of central importance in high level fuel cycle analyses done to determine the effects of different fuel cycle options.

The isotope composition of reactor fuel depends on the spatial and spectral distribution of neutrons in the core and many large software packages exist that generate these flux profiles [1–4]. Most do so by solving approximations to the neutron diffusion or transport equations and the various methods by

* Corresponding author. Fax: +1 206 300 4147.
*E-mail address:* mrd6@cornell.edu (M.R. Deinert).

0022-3115/$ - see front matter © 2006 Elsevier B.V. All rights reserved.
doi:10.1016/j.jnucmat.2006.04.012

which this is done are discussed in several texts [5–8]. A traditional approach for solving a burnup problem would use one of the software packages mentioned above to produce few- or one-group cross sections amenable to ORIGEN2 burnup calculations. ORIGEN2 would then be used to take a burnup step of a few MWd/kg, at which time one-group cross sections, and hence the spectrum, would be re-computed. This technique, while somewhat cumbersome, is of great value for high-fidelity burnup calculations. However, a simplified approach for calculating the spatial and spectral neutron distribution in a reactor using a small number of input parameters with minimum setup and execution time, and amenable to tracking isotope concentrations over the lifetime of a fuel batch, is missing from the literature.

Most neutronics packages compute the energy dependence of the neutron flux using one of two methods. A multigroup formulation is often employed in which the energy spectrum is discretized into tens or hundreds of groups [9–11]. The flux, nuclear cross sections and group-to-group transfer functions are averaged over each group in a manner that aims to preserve the correct within-group interaction rate. The energy-dependent equation of neutron conservation is then written as a set of coupled algebraic equations. Typically the control absorber concentration is iterated upon, or the multiplication factor, $k_{\text{eff}}$, is treated as an eigenvalue. Alternately, a continuous method is sometimes employed which aims to avoid complications that arise in calculations involving discontinuous functions such as the scattering kernel [12]. The idea is to formulate approximate differential equations for a smooth, slowly varying slowing-down density, $q$ [n/cm$^3$/s].

Available neutronics packages often compute the spatial dependence of the neutron flux using 'nodal methods' in which the reactor is divided into macroscopic regions, i.e. nodes, for which detailed calculations of the flux distribution are carried out [9–11]. Nodes of a similar type are often assumed to have similar flux profiles and boundary values between adjacent nodes are matched to preserve continuity. Codes typically use finite differencing to spatially discretize the nodes, and then implement either an approximation to the diffusion [13] or transport equations [10]. A necessary condition for stability is that the grid spacing be smaller than a length scale characterized by the shortest group mean free path which can be the order of 1 cm when the diffusion equation is being discretized. Because of this, it is often impractical to solve for the full three-dimensional flux profile via finite difference methods. Typically the dimensionality of the problem is reduced, via the definition of an equivalent 1-d or 2-d problem, or a 3-d calculation is performed over only a small spatial region. If the transport equation is being implemented 'discrete ordinates' techniques are used to discretize its angular dependence, evaluating it at only a few set directions (ordinates) [12]. Quadrature is then used to reproduce the full equation.

Monte Carlo packages offer an alternate method for determining both spatial and spectral neutron distributions in a reactor core [14]. Here, neutron histories are directly simulated from birth, usually via isotropic emission from fission. The fission source is generated by sampling a Bayesian statistical distribution in the energy, position and direction variables. A neutron is followed from birth, through the slowing down process, until its final absorption or escape. Treatment is as exact as the geometric and physical inputs allow. Naturally, a large (and problem-dependent) number of histories must be generated to reduce variance to within specified guidelines. Variance reduction may be accelerated by attaching weights to individual neutron histories and is often carried out on the basis of an adjoint or importance function obtained beforehand by deterministic means.

We consider a different approach from the above where the spatial dependence of the neutron flux is computed using a combination of collision probability and equivalence theory. This rests on the premise that detailed spatial variations in the neutron flux are unimportant provided that average cross sections, $\langle\Sigma\rangle$, and fluxes, $\phi_{\text{ave}}$, can be derived that preserve interaction rates within macroscopic regions. The condition imposed by equivalence theory is that, over a large heterogeneous region $V$

$$\langle\Sigma\rangle\phi_{\text{ave}} = \frac{1}{V}\int_V \mathrm{d}V\,\Sigma(r)\phi(r). \tag{1}$$

Collision probability theory then models the transport of neutrons from region-to-region using transmission and escape probabilities. The overall aim is to reduce the spatial dependence of the problem to that of only a few regions. Such an approach was used in the WIMSD-5 code developed by the British [15] and was intended primarily for static neutronics calculations on thermal reactors. We extend this approach to consider the time dependence of the spatial and energy-dependent neutron

flux in a reactor core in a way that is amenable to rapid computation on a PC. The concentration of 24 actinides is tracked through time and the model accepts as inputs fuel element geometry and composition, moderator/coolant geometry and composition, reactor geometry, fuel residence time and target discharge burnup.

## 2. Methods: Overview

In order to simplify analysis, the spatial and spectral dependence of the neutron transport equation are decoupled and the energy spectrum is modeled using a multigroup formulation. The reactor itself is viewed as being comprised of two regions, fuel and moderator/coolant, with the movement of neutrons from one to the other accounted for using escape and transmission probabilities. Within each region the flux is assumed to take on an average value which considerably simplifies the analysis. The objective then is not to accurately model the spatial dependence of the flux, but instead its energy spectrum and through this the time dependent concentration of isotopes in the reactor as a whole. Two methods are available for modeling reactivity control. A burnable poison may be introduced in the fuel, and/or the model may adjust a time-dependent, system-wide control absorber to achieve criticality.

The resulting model is demonstrated with a calculation of the neutron spectrum for a reactor with the specifications given by the 1994 Burnup Credit Criticality Benchmark compiled by the Organization for Economic Cooperation and Development along with the Nuclear Energy Agency [16].

### 2.1. Decoupling the spatial and spectral dependence of the neutron transport equation

The neutron transport equation can be written

$$\begin{aligned}\Omega\cdot\nabla\phi(r,E,\Omega)+\Sigma_{\mathrm{t}}\phi(r,E,\Omega)&=\int_{4\pi}\mathrm{d}\Omega'\int_0^{\infty}\mathrm{d}E'\Sigma_{\mathrm{s}}(r,E'\to E,\Omega'\to\Omega)\phi(r,E,\Omega')\\&\quad+\frac{\chi(E)}{4\pi}\int_0^{\infty}\mathrm{d}E'\upsilon\Sigma_{\mathrm{f}}(r,E')\phi(r,E').\end{aligned}\tag{2}$$

Here $\Omega$ is the directional vector [ster], $r$ the positional vector [cm], $\phi(r,E,\Omega)$ is the neutron flux per unit energy per unit solid angle [n/cm$^2$/ster/eV/s], $\phi(r,E)$ is the neutron flux per unit energy [n/cm$^2$/s], $\Sigma_{\mathrm{t}}(r,E,\Omega)$ is the total macroscopic cross section [1/cm], $\Sigma_{\mathrm{s}}(E'\to E,\Omega'\to\Omega)$ is the scattering cross section from $(E',\Omega')$ into $(E,\Omega)$ [1/cm/eV/ster], $\Sigma_{\mathrm{f}}(r,E')$ is the macroscopic fission cross section per unit energy [1/cm/eV], $\chi(E)$ is the probability per unit energy that a fission neutron will be born at energy $E$ [1/eV] and $\nu(r,E)$ is the neutron yield per fission.

In practice, the transport equation is formulated as a set of coupled integro-differential equations. To reduce the problem of solving these it is necessary to decouple the spatial and energy variables, this is done by removing the angular dependence of the flux in Eq. (2). For purposes of energy transfer, we preserve the isotropic and linearly anisotropic components of the elastic scattering kernel in the center-of-mass system. In order to decouple space and energy in the transport equation, we adopt the simplest approximation, replacing the total cross section with a transport cross section of the form

$$\Sigma_{\mathrm{tr}}=\Sigma_{\mathrm{a}}+(1-\bar{\mu})\Sigma_{\mathrm{s}},\tag{3}$$

where $\mu$ is the average value of the cosine of the scattering angle. Hence, scattering events devolve into a neglected forward component and an isotropic component governed by $\Sigma_{\mathrm{tr}}$. Values of $\mu$ are readily obtainable from the Evaluated Nuclear Data File (ENDF) data base maintained by the National Nuclear Data Center, Brookhaven National Laboratory.

To model the transport of neutrons between the fuel and moderator/coolant, an effective cell consisting of a homogeneous fuel element surrounded by a region of moderator/coolant is constructed. The spatial dependence of the flux is treated by taking the neutron number density in the respective fuel and moderator/coolant regions to be uniform. This simplification greatly facilitates spatial transport computations, as it allows us to apply the reciprocity theorem (see below). It is important to emphasize that the goal is not to accurately model the spatial dependence of the flux, but instead its spectral dependence and through this the time dependent concentration of isotopes in the reactor as a whole.

The transport of neutrons between regions is then governed by transmission and escape probabilities, themselves functions of energy, which are defined in Table 1. Using these, we let $\Pi_0$ be the probability that a neutron appearing in the fuel at energy $E$ will undergo its next interaction in the moderator/coolant

Table 1
Definition of escape and transmission probabilities

| Term | Definition | Assumptions |
|---|---|---|
| $P_0$ | Probability that a neutron, having has its last interaction in the fuel, will escape the fuel without further interaction | Uniform isotropic source black moderator region |
| $T_0$ | Probability that a neutron entering the fuel region is transmitted without interaction | Cosine surface source at boundary black moderator region |
| $P_1$ | Probability that a neutron, having had its last interaction in the moderator, will escape the without further interaction | Uniform isotropic source black fuel pin |
| $T_1$ | Probability that a neutron entering the moderator is transmitted without interaction (Dancoff factor) | Cosine surface source at boundary black fuel pin |

Definition of the respective probabilities for the transport of neutrons between fuel and moderator/coolant.

$$\Pi_0 = P_0(1-T_1) + P_0T_0T_1(1-T_1) + \cdots = \sum_{m=0}^{\infty} P_0(1-T_1)(T_0T_1)^m = P_0(1-T_1)\frac{1}{1-T_0T_1}. \tag{4}$$

Similarly, $\Pi_1$ is the probability that a neutron of energy $E$ appearing in the moderator undergoes its next interaction in the fuel

$$\Pi_1 = P_1(1-T_0)\frac{1}{1-T_0T_1}. \tag{5}$$

It can be shown [6] that $\Pi_1$ and $\Pi_0$ satisfy a reciprocity relationship of the form

$$\Pi_0 V_0 \Sigma_0 = \Pi_1 V_1 \Sigma_1, \tag{6}$$

where $V_i$ is the volume of region $i$ ('0' for fuel, '1' for moderator/coolant) and $\Sigma_i$ is the (spatially averaged) macroscopic total cross section within the respective region. We observe that this relationship obviates the need to separately calculate $P_1$.

The relationship between $\Pi_0$ and $\Pi_1$ and the transmission and escape probabilities can alternatively be obtained for an arbitrary lattice structure as outlined below. This derivation shows that one can, in theory, relax the assumptions of uniform source and flux distributions within the regions. This also implies that successive transmissions through fuel and moderator need not have the same $T_0$ and $T_1$. Consider the element pictured in Fig. 1. Monoenergetic sources are distributed in Region 0 of this element. The sources can be thought of as stemming from fission and/or inscattering to the energy being considered. The neutron currents $J_+$ and $J_-$ [n/cm$^2$/s] at the interface are defined in the usual way, and we denote the rates [n/s] at which neutrons cross the interface by $\langle J_+A\rangle$ and $\langle J_-A\rangle$. Similarly the rate of neutron production [n/s] is written as $\langle S_0V_0\rangle$. Then, it follows from the definitions of $P_0$ and $T_0$ that

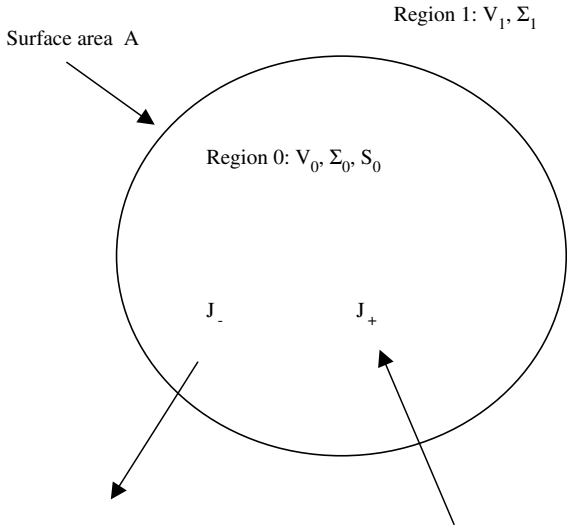


Fig. 1. A conceptual unit cell.

$$\langle J_+A\rangle = \langle S_0V_0\rangle P_0 + \langle J_-A\rangle T_0 \tag{7}$$

and

$$\langle J_-A\rangle = \langle J_+A\rangle T_1. \tag{8}$$

Likewise, the definition of $\Pi_0$ implies that

$$\langle S_0V_0\rangle \Pi_0 = \langle J_+A\rangle - \langle J_-A\rangle. \tag{9}$$

This equates the production rate of neutrons in Region 1 multiplied by the probability that a neutron born in Region 0 will experience its next interaction in Region 1 to the net number of neutrons per second crossing the boundary between the regions. Treating $\langle J_+A\rangle$, $\langle J_-A\rangle$ and $S_0V_0$ as independent variables, we write the above system as

$$\begin{bmatrix} P_0 & T_0 & -1 \\ 0 & -1 & T_1 \\ \Pi_0 & 1 & -1 \end{bmatrix} \begin{pmatrix} \langle S_0V_0\rangle \\ \langle J_-A\rangle \\ \langle J_+A\rangle \end{pmatrix} = \begin{pmatrix} 0 \\ 0 \\ 0 \end{pmatrix}. \tag{10}$$

For a solution to exist, the determinant of the matrix of cofactors must be zero, from which equation (4) immediately follows. The derivation of $P_1$ is analogous if one instead places the source $\langle S_1 V_1 \rangle$ in Region 1. In practice, the difficulty of calculating the $P$ and $T$ probabilities limits one to simple geometries and/or uniform source distributions. Our approach is discussed in the following section.

Neutron leakage is handled by use of an absorptive term of the form $D(E)B^2\phi(E)$, where $D$ [cm] and $B^2$ [1/cm$^2$] are the effective diffusion coefficient and geometric buckling of the reactor. A uniformly distributed control absorber can be used to keep the reactor in the critical configuration. Note that the control absorber concentration for this pin-cell model is conceptually different from that of a critical reactor, as it models neutron sharing between fresh and depleted fuel as well as criticality control.

It is now possible to recast the transport equation in an approximate form where the spatial and energy variables have been decoupled. The governing equations for the energy-dependent fluxes in the fuel and moderator/coolant regions are coupled via the probabilities $\Pi_0$ and $\Pi_1$ and can be written

$$\begin{aligned}
&[\Sigma_0(E) + D(E)B^2]\phi_0(E) \\
&\quad = (1 - \Pi_0(E))\left[\int_0^\infty \mathrm{d}E'\phi_0(E')\Sigma_{\mathrm{s},0}(E' \to E)\right. \\
&\qquad \left. + \chi(E)\int_0^\infty \mathrm{d}E'\phi_0(E')\nu_0(E')\Sigma_{\mathrm{f},0}(E')\right] \\
&\qquad + \frac{V_1}{V_0}\Pi_1(E)\left[\int_0^\infty \mathrm{d}E'\phi_1(E')\Sigma_{\mathrm{s},1}(E' \to E)\right. \\
&\qquad \left. + \chi(E)\int_0^\infty \mathrm{d}E'\phi_1(E')\nu_1(E')\Sigma_{\mathrm{f},1}(E')\right] \qquad (11)
\end{aligned}$$

and

$$\begin{aligned}
&[\Sigma_1(E) + D(E)B^2]\phi_1(E) \\
&\quad = (1 - \Pi_1(E))\left[\int_0^\infty \mathrm{d}E'\phi_1(E')\Sigma_{\mathrm{s},1}(E' \to E)\right. \\
&\qquad \left. + \chi(E)\int_0^\infty \mathrm{d}E'\phi_1(E')\nu_1(E')\Sigma_{\mathrm{f},1}(E')\right] \\
&\qquad + \frac{V_0}{V_1}\Pi_0(E)\left[\int_0^\infty \mathrm{d}E'\phi_0(E')\Sigma_{\mathrm{s},0}(E' \to E)\right. \\
&\qquad \left. + \chi(E)\int_0^\infty \mathrm{d}E'\phi_0(E')\nu_0(E')\Sigma_{\mathrm{f},0}(E')\right], \qquad (12)
\end{aligned}$$

where the numerical subscripts again refer to the spatial regions, $V$ is the volume region [cm$^3$] and all other terms are as previously defined. Note that Eqs. (11) and (12) allow for the possibility of fission occurring in the annular, rather than the central region, a situation that would occur with a reactor such as the GT-MHR.

### 2.2. Fuel and moderator/coolant escape and transmission probabilities

The energy-dependent transport probabilities $\Pi_0$ and $\Pi_1$ are defined in Eqs. (4) and (5) in terms of region-to-region escape ($P_0$ and $P_1$) and transmission ($T_0$ and $T_1$) probabilities. These may be formulated in terms of geometric and material properties as outlined below.

$T_0$ and $P_0$: The probability that a neutron entering the fuel will be transmitted without interaction, $T_0$, can be determined using a cosine-distributed point source at the boundary of the fuel region. This point source represents the neutrons entering the fuel from the moderator. We derive $T_0$ by calculating the fraction of neutrons that pass through the pin without incident. The transmission probability can then be written

$$T_0 = \frac{S/2 - \int_V \mathrm{d}V\Sigma\phi(\rho')}{S/2}, \qquad (13)$$

which is found to be a function of the dimensionless fuel pin thickness, $\Sigma d$, where $\Sigma$ is the transport cross section within the pin and '$d$' is a characteristic length, i.e. thickness for a plate, diameter for a sphere or cylinder. Closed-form expressions for $T_0$ can be obtained for each of these geometries.

The probability that a neutron, having had its last interaction in the fuel, will escape to the moderator/coolant, $P_0$, is then given by the reciprocity relationship

$$1 - T_0 = \frac{4V\Sigma}{A}P_0, \qquad (14)$$

where $V/A$ is $t/2$ for plates, $r/2$ for cylinders and plates and $r/3$ for a spheres and '$r$' is the fuel pin radius [cm] and '$t$' is thickness [cm]. For an infinite cylindrical fuel pin of radius '$r$', and $a = \Sigma r$, it can be shown that $P_0$ is well approximated by

$$P_0 = \frac{1 + (c + 2/3)a + 8/3ca^2}{1 + (c + 2)a + (2c + 4/3)a^2 + 16/3ca^3}, \qquad (15)$$

where '$c$' is a fitting parameter. Eq. (15) goes to $1 - a(4/3)$ as '$a$' goes to zero and to $1/(2a) - 3/(32a^3)$. The use of Eq. (15), a rational approximation, is computationally inexpensive and introduces negligible error. A value of $c = 0.3567$ gives $P_0$ its exact value of 0.40715 [17] at $a = 1$.

$T_1$ and $P_1$: The probability that a neutron entering the moderator/coolant from the fuel will be transmitted without interaction and thus re-enter a fuel pin, $T_1$, is known as the Dancoff factor. Except for the case of slab geometry, computation of $T_1$ is considerably more involved than that of $P_0$ or $T_0$, since the moderator/coolant region of a lattice is not convex.

The original work in this area treated the problem in a general manner, resulting in tabulation of the Dancoff factor for parallel circular cylinders as a function of two dimensionless parameters: the pin radius to pitch ratio, $B = r/p$, and the pin radius measured in moderator mean free paths, $a = \Sigma_1 r$ [18]. The shortcoming of these tabulated values is that they quantify nearest-neighbor rod-shadowing effects only. Especially in the case of high-energy neutrons, where the mean free path in the moderator is large compared to the pitch, this shortcoming results in substantial error.

The most commonly pursued strategy for accurate computation of $T_1$ is Monte Carlo integration over all neutron trajectories. Several code packages are in use to perform this calculation [19]. We have also developed a Monte Carlo code for cylindrical geometries that closely reproduces the results of other codes [20] but with computational savings [21]. A plot of the Dancoff factor, for cylindrical pins in a square lattice, as a function of $\Sigma r$ and $V_1/V_0$, applicable to the test case used in this study is shown in Fig. 2. Here $V_1/V_0$ (the hydraulic radius) is twice the volume to surface ratio of the moderator region [21].

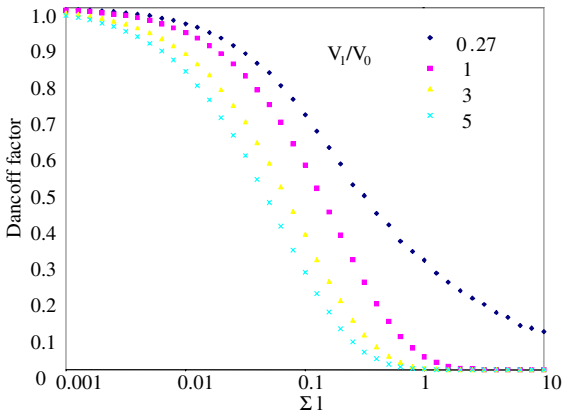


Fig. 2. Dancoff factor. The Dancoff factor for different fuel cell fuel pin to moderator volume ratios are shown. Here '$l$', the hydraulic radius, is twice the volume to surface ratio of the moderator region [Barratt, 2003].

Three of the four probabilities are thus determined by closed-form or Monte Carlo analysis. The fourth, $P_1$, is the probability that a neutron which had its last interaction in the moderator is transmitted to the fuel without further interaction. This can be determined using the reciprocity relationship of Eq. (6).

### 2.3. Determining the lethargy dependent flux

Using the multigroup formulation, we discretize the energy spectrum into $N$ groups. It is useful to reformulate the problem in terms of the lethargy $u$

$$u = \ln \frac{E}{E_0}, \tag{16}$$

where $E_0$ is chosen to be the upper boundary of the highest-energy group. Since over 99% of fission neutrons are born at $E < 10$ MeV, we take $E_0 = 10$ MeV as a practical upper boundary for our calculations. We divide lethargy space into two conceptual regions: the epithermal/fast region (hereafter referred to as 'fast'), into which fission neutrons are born and resonance absorption predominates, and the thermal region, where energy gain via upscattering becomes significant. Since no appreciable upscattering occurs for neutrons with energies greater than 1 eV, we choose this as a cutoff between the two regions.

Several energy discretization structures are currently in common use [22]. For fast reactors, or when fine resolution is desired in the epithermal region, the LANL-70, CSEWG or VITAMIN-E group structures are often employed. Structures intended to address the thermal region include EPRI-CPM 69-group and LASER-THERMOS. Two examples of more comprehensive structures that span the entire energy range of interest in reactor physics are LANL-187 and GAM-II. The bulk of these structures were laid out to address neutron spectra arising in specific reactor types, or to thoroughly treat resonance absorption in one or more nuclides of particular interest. In order to preserve the general applicability of the current model, we select a very fine group structure in the fast region and coarser one at low energies. In this way the model maintains sufficient resolution to handle the resonance absorbers whose presence might not be known a priori. The initial group spacing is chosen to be $\Delta u = 0.2303$ in the thermal region and $\Delta u = 0.02303$ at higher energies, Fig. 3. However, this hyperfine structure is not maintained through an

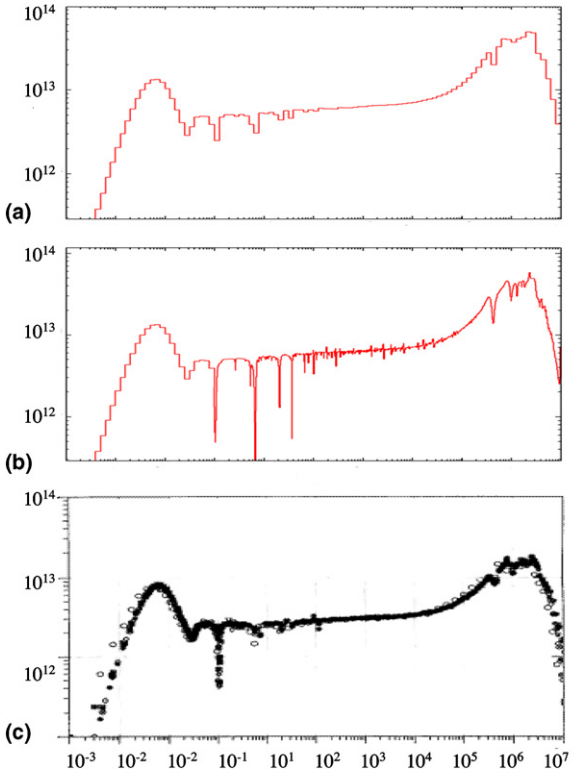


Fig. 3. Neutron flux vs lethargy. (a,b) The end of life neutron spectra from this model for case 7 of the IA Benchmark with a course group structure (a) and a fine group structure (b). (c) The spectra from the IA Benchmark showing data from 14 different international groups. The lethargy scale is shown at the bottom of (c) and the vertical axis' are neutron flux [n/cm$^2$/s]. The vertical scale for (c) was reported in 'arbitrary units' and was multiplied by $10^{14}$ to make it consistent with (a,b). The difference between (a,b) and (c) is the result of differences in group structures employed in the simulations.

entire calculation, rather it is coarsened based upon the results of a single sweep in energy to become $\Delta u = 0.2303$ in the fast region as well.

In both the thermal and fast regions, we define a groupwise flux [n/cm$^2$/s] for group $g$ as

$$\phi_g = \int_g \mathrm{d}u \phi(u), \tag{17}$$

where subscripts denoting spatial regions have been dropped for clarity. In most cases we can assume a flux profile constant in lethargy far from isolated resonances, and since our group structure is relatively fine, this choice does not have a large impact on the numerical value of the group constants themselves.

Other group averaged quantities of importance to the current model are

$$S_g = \frac{\int_g \mathrm{d}u S(u)\phi(u)}{\phi_g} \tag{18}$$

and

$$K_{g'\to g} = \frac{\int_{g'} \mathrm{d}u' \int_g \mathrm{d}u K(u' \to u)\phi(u')}{\phi_g}, \tag{19}$$

where $S$ is a cross section or other array of pointwise values in lethargy ($\Sigma$, $\Sigma_a$, $\nu$, etc.) and $K$ is any kernel, i.e. $\Sigma_s(u' \to u)$. For cross sections, these definitions are seen to preserve the correct interaction rates. The effective diffusion coefficient for a group is calculated for the homogeneous reactor (i.e., with the two spatial regions 'smeared') by

$$D_g = \left( \frac{(V\phi)_0 + (V\phi)_1}{3[(V\phi\Sigma)_0 + (V\phi\Sigma)_1]} \right)_g \tag{20}$$

in which we have returned to use the numerical subscripts to denote spatial regions in the reactor and $\Sigma$ is obtained using Eq. (15).

Calculation of self-shielded resonance cross sections is of critical importance in determining neutron spectra in both fast and thermal reactors. The present model addresses both types of spectra, and is intended to treat a broad range of fuel compositions and temperatures, which complicates the computation of these cross sections. Hence we choose to treat group-averaged cross sections in the resonance region as being functions of two parameters, the temperature and a background cross section $s$ [barns per resonance absorber atom] that quantifies the dilution of the resonance absorber. The dependence of a group constant $\sigma_g$ on these quantities is captured by the self-shielding $f$-factor [22]

$$f = \frac{\sigma(T,s)}{\sigma(T, s \to \infty)}. \tag{21}$$

Both $\sigma(T,\infty)$ and $f(T,s)$ are then tabulated, for a number of temperatures and background cross sections, from the ENDF database using NJOY, with $f(T,s)$ calculated in a manner consistent with the Bondarenko method [23]. Our choice of a group structure reduces any error that might be induced due to the inaccuracy of this weighting function appropriate for the reactor type and fuel composition being considered.

In its simplest form, the Bondarenko model smears the fuel pin geometry into a single spatial region, so that, if $N$ nuclides are present, the background cross section for the $i$th nuclide, $s_i$, can be written

$$s_i = \frac{1}{\alpha_i}\sum_{k\neq i}^{N}\alpha_k\sigma_k. \tag{22}$$

Here $\alpha^k$ is the atom fraction of the $k$th nuclide and $\sigma^k$ is its total microscopic cross section. We may generalize this expression to be consistent with our two spatial region formulation by defining a macroscopic escape cross section $\Sigma_{e0}$ in terms of the probability $\Pi_0$ as

$$\Pi_0 = \left(\frac{\Sigma_e}{\Sigma_e + \Sigma}\right)_0. \tag{23}$$

A macroscopic escape cross section $\Sigma_{e1}$ for neutrons born in Region 1 may be analogously defined. Observe that we can write the microscopic escape cross section $\sigma_{e0}$ as

$$\sigma_{e0} = \left(\frac{\Pi}{1-\Pi}\right)_0\sigma_0 = \left(\frac{\Pi}{1-\Pi}\right)_0\sum_{k}^{N}\alpha_k\sigma_k, \tag{24}$$

where the sum is carried out over all nuclides in Region 0, including the resonance absorber. The background cross section given in (22) may then be written for the two region formulation as

$$s_{i,0} = \frac{1}{\alpha_{i,0}}\left(\sigma_e + \sum_{k\neq i}^{N}\alpha_k\sigma_k\right)_0. \tag{25}$$

Now the summation is carried out only over the nuclides in Region 0. The escape cross section is seen to simulate the presence of another background absorber, capturing the effect of interactions taking place in Region 1. Combining (24) and (25) leads to the final expression for the background cross section perceived by the $i$th nuclide in Region 0

$$s_{i,0} = \left(\frac{\Pi}{1-\Pi}\sigma_i + \frac{1}{\alpha_i}\sum_{k\neq i}^{N}\frac{1}{1-\Pi}\sigma_k\alpha_k\right)_0. \tag{26}$$

An analogous expression pertains to the background cross sections perceived by any resonance absorbers present in Region 1.

This escape probability formulation thus introduces the group averaged cross section of the resonance absorber into the equation for the background cross section it experiences. Also some of the other nuclides whose cross sections appear in Eq. (26) may themselves be resonance absorbers, and the probabilities $\Pi_0$ and $\Pi_1$ are themselves functions of the resonance absorber cross sections. A simple iterative scheme, in which all resonance absorbers are initially assumed to be present at infinitely dilute concentration for the initial calculation of $\Pi_0$ and $\Pi_1$, is used. This scheme has been found to converge very quickly in practice.

To account for neutron leakage from the core, we use the well-known approximation from diffusion theory, that leakage is proportional to an effective diffusion coefficient and the reactor geometric buckling. Reactors are generally configured as square cylinders. However, even if an infinite reflector thickness is assumed, calculation of the buckling is a laborious procedure. Therefore, we choose to obtain the geometric buckling for an infinitely reflected spherical reactor of the same volume as the actual, cylindrical reactor, see [Lamarsh], for a discussion of the validity of this assumption.

Using the multigroup formalism, and assuming that fissions only occur in the fuel, we can now write Eqs. (11) and (12) as a set of coupled, linear algebraic equations in lethargy

$$\begin{aligned}(\Sigma_0 + DB^2)_i\phi_{0,i} &= (1-\Pi_{0,i})\left[\sum_{j=1}^{N}\Sigma_{s,0}(j\to i)\phi_{0,j} + R\chi_i\right] \\ &\quad + \frac{V_1}{V_0}\Pi_{1,i}\sum_{j=1}^{N}\Sigma_{s,1}(j\to i)\phi_{1,j}\end{aligned} \tag{27}$$

and

$$\begin{aligned}(\Sigma_1 + DB^2)_i\phi_{1,i} &= \frac{V_0}{V_1}\Pi_{0,i}\left[\sum_{j=1}^{N}\Sigma_{s,0}(j\to i)\phi_{0,j} + R\chi_i\right] \\ &\quad + (1-\Pi_{1,i})\sum_{j=1}^{N}\Sigma_{s,1}(j\to i)\phi_{1,j},\end{aligned} \tag{28}$$

where we have replaced the fission source terms with a discretized probability distribution (denoted by $X_i$ and subject to the condition that the sum over $X_i = 1$) with $R$ being the neutron birth rate per unit volume. Numerical subscripts again refer to spatial regions, '$i$' and '$j$' denote respective group numbers.

Eqs. (27) and (28) are then implemented with a 110 group structure labeled in order of increasing lethargy. We are thus confronted with solving $2N$ coupled algebraic equations that are linear in the $\phi$ with the coupling present in many parameters: $\Sigma_s$ and $X_i$, the diffusion coefficient $D$ and the probabilities $\Pi_i$.

For groups 1 through 70 (i.e. $E > 1$ eV), we have a triangular system of equations with known source terms. These may be solved successively. The equa-

tions describing the thermal spectrum (groups 71 through 110) are solved separately, with the source terms written to include inscattering from the high-energy groups. In this energy regime ($E < 1$ eV), the isotopic scattering kernels include significant upscattering components as well as, in some cases, lattice effects. Therefore, we assemble groupwise scattering transfer functions from ENDF $S(\alpha, \beta)$ data as processed by the NJOY THERMR and GROUPR modules. The resultant $80 \times 80$ system of densely coupled equations is solved by LU decomposition.

Once the calculation is complete, we have obtained the flux distribution for the assumed value of the volumetric neutron production rate, $R$. This solution can be iterated on the control absorber concentration until the number of fission neutrons produced is in fact equal to $R$; a procedure that is equivalent to imposing the condition $\rho = 0$. This computation iteratively updates the control absorber concentration until the criticality condition

$$\sum_{i=1}^{N} (\nu \Sigma_f \phi)_i = R \tag{29}$$

is satisfied. Near the end of fuel residence time, it is possible for Eq. (20) to imply a negative control absorber concentration. Physically this corresponds to a local multiplication constant that is less than one: the burned-out fuel pin being modeled 'borrows' neutrons from adjacent fresher fuel for the chain reaction to be maintained. When such a scenario holds, we fix the control absorber concentration to be zero and allow the local reactivity to become negative.

### 2.4. Benchmarking of results

For over a decade the criticality working group of the Nuclear Energy Agency (NEA) has researched the methods and data required for calculation of burn-up credit in criticality safety. In 1994 and 2003 a series of benchmark standards were published for simulations in UOX and MOX burning LWRs which appear in the subsequent OECD/NEA Phase 1A and Phase IVA, B reports [16,24]. In all cases a benchmark standard which specified geometry, fuel make up, water density and other relevant parameters was outlined by the NEA and various institutions from around the world were solicited to submit simulations showing results such as isotopic composition, $k_{inf}$, and reaction rates. We describe the individual benchmark studies briefly, referring the reader to the reports for the details of each benchmark case.

The Phase 1A report considered a UOX benchmark problem, with an infinite array of simple PWR unit cells [16]. The simulations were performed for burnups of 30 and 40 MWd/t with 1 and 5 years of cooling time. Fifteen fission products (FP) were tracked along with the actinides U-234, 235, 236, 238; Pu-238, 239, 240, 241, 242; Am-241, 243 and Np-237, with $k_{inf}$ also reported. The average of the results from the 25 submitted simulations were provided along with the relevant standard deviations. We compare simulations done with our code to the results presented for cases 1, 4 and 5 of the benchmark study.

The Phase IV-A benchmark calculated infinite PWR fuel pin-cell reactivity for fresh and irradiated fuels in full MOX cores. The study considered the impact of different initial plutonium isotopic compositions in the MOX fuel associated with first-generation MOX, weapons plutonium and multiple MOX recycle. Simulations were done for burnups of 20, 40 and 60 MWd/t with cooling periods of one and five years. Thirty-seven simulations were submitted to the Phase IV-A benchmark, which reports their average and standard deviation. The benchmark study reported only $k_{inf}$ and we compare results obtained with our code to those presented for core cases 1, 10, 20, 29, 39 and 51.

The Phase IV-B benchmark considered MOX fuels that would be irradiated in a mixed UO2-MOX PWR core, alongside UO2 fuel assemblies with an initial enrichment of 4.3 w/o U-235 /U [24]. Two plutonium vectors were considered, one appropriate to typical plutonium derived from reprocessed thermal reactor UO2 fuels and another appropriate to plutonium from dismantled weapons. Each plutonium vector was considered in a supercell calculation for a MOX assembly together with three UO2 fuel assemblies, a MOX-only core representation with reflective boundary conditions and a simple MOX pin-cell calculation (using the average MOX fuel composition) with pin-cell geometry that conserves the fuel-to-moderator ratio of the whole assembly with reflective boundary conditions. We compare results only with the latter case. The study tracked isotope concentrations as well as $k_{inf}$ and gave temporal data for the major uranium, plutonium, americium and curium isotopes. The results reported were the averages and standard deviations from the nine submitted simulations.

## 3. Results and discussion

Figs. 4–6 show a comparison of the isotopic prevalence vs burnup for Cm-242, Np-237, Am-243, 242m, 241, Pu- 242, 240, 241, 238 and 239 as given by the present model, MONTEBURNS and the OECD/NEA Phase IV-B benchmark. The error bars in the figures correspond to the standard deviations for data presented in the latter study. As can be seen the present model shows strong fidelity to the homogeneous core benchmark values in all cases and gives results that are within the standard deviations for the OECD/NEA values for every isotope except Pu-241, for which it is close. Figs. 4–6 are representative of the correspondence between the present model and the Phase IV-B benchmark results for all 24 isotopes that it tracks.

Table 2 shows a comparison of the $k_{inf}$ values for cases 1, 4 and 5 of the OECD/NEA Phase 1A benchmark with those given by this model along with benchmark standard deviations. Table 3 shows a comparison of the $k_{inf}$ values for cases 1, 10, 20, 29, 39 and 51 of the Phase 4A benchmark with those given by this model along with benchmark standard deviations. As with the time dependent isotope prevalence, the results are very close in all cases. Table 4 shows a comparison of the Phase 1A endpoint isotope concentrations (at 40 MWd/kg) as compared with those predicted by the present model. All values are within 13% of the OECD/NEA results and while no standard deviations were given for the latter data, Figs. 2–6 suggest that the results given by the present model would fall within this range.

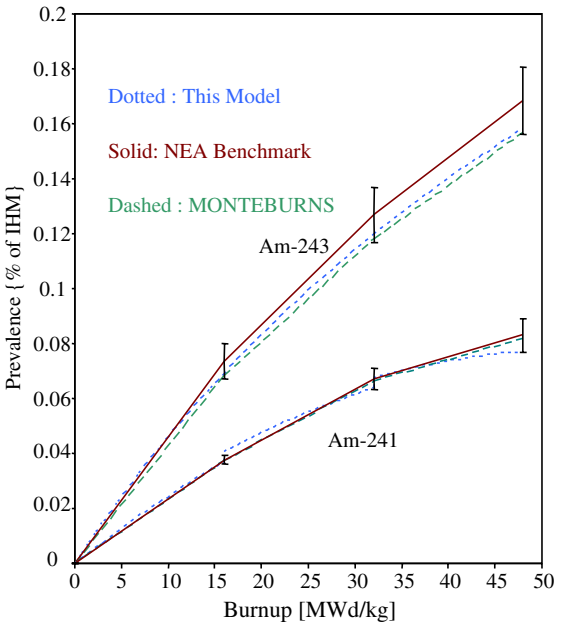


Fig. 4. Am-241 and Am-243 prevalence. The prevalence of Am-241 predicted with this model and compared with NEA benchmark and a MONTEBURNS simulation along with the prevalence of Am-243 predicted with this model and compared with NEA benchmark and a MONTEBURNS simulation. The standard deviations represent those for the relevant averages from the NEA benchmark.

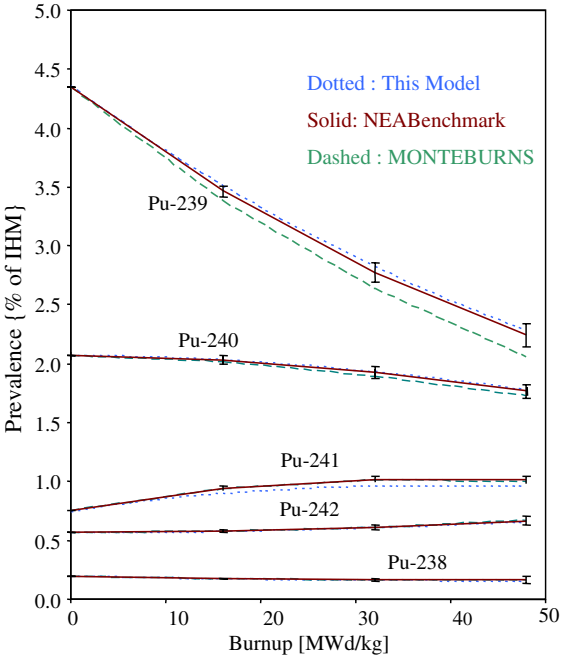


Fig. 5. Pu-238–242 prevalences. The prevalence of plutonium species as predicted with this model and compared with NEA benchmark and a MONTEBURNS simulation. The standard deviations represent those for the relevant averages from the NEA benchmark. In all cases the current model gives predictions that are in close agreement with those of the NEA benchmark.

By creating a two region model of a nuclear reactor core that uses collision probability approximations to the neutron transport equation we were able to determine the energy-dependent neutron flux in a manner that preserves the overall interaction rate within the core. Comparison of results from this model with data from the OECD/NEA benchmark criticality studies, and with simulations done using MONTEBURNS, shows a very high degree of fidelity for homogenous core loadings. This, coupled with a run time of 30 seconds or less on a 1 GHz Pentium based computer, make the present model an excellent choice for high level analyses of nuclear fuel cycles. Because of its restricted spatial resolution, however, it would not be applica-

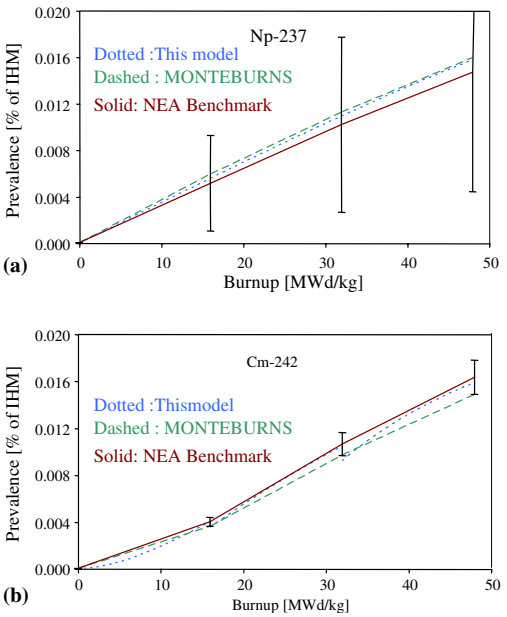


Fig. 6. Np-237 and Cm-242 prevalence. (a) Prevalence of Np-237 predicted with this model and compared with NEA benchmark and a MONTEBURNS simulation. (b) Prevalence of Cm-242 predicted with this model and compared with NEA benchmark and a MONTEBURNS simulation. The standard deviations represent those for the relevant averages from the NEA benchmark.

Table 2
Phase 1A $k_{inf}$ values compared with those obtained with our model

| $k_{inf}$ | This model | OECD | Diff | $2^*\sigma$ |
|---|---|---|---|---|
| $k_{inf}$ (Case 1) | 1.445 | 1.439 | 0.006 | 0.017 |
| $k_{inf}$ (Case 4) | 1.255 | 1.246 | 0.009 | 0.011 |
| $k_{inf}$ (Case 5) | 1.199 | 1.188 | 0.011 | 0.012 |

The standard deviation for the OECD results is $\sigma$.

ble to fuel management simulations in which the composition and reactivity of individual fuel rods is important. In its present form, it is also not applicable to certain heterogeneous fuel loadings where internodal coupling dominates the neutron number density and energy distribution in a given pin. However, less strongly heterogeneous systems (such as assembly wise heterogeneous MOX or inert matrix fuel loadings) have yielded good results using the homogenized idealization [25]. Indeed, this idealization finds widespread use in sophisticated reactor burnup packages such as the COSI system used by the Commissariat l'Energie Atomique in France [26].

Table 3
Phase 1A endpoint isotope concentrations (at 40 MWd/kg) compared with those obtained with our model

| Isotope | This model | OECD | % Diff |
|---|---|---|---|
| U235/U | 8.383E−03 | 8.460E−03 | −0.91 |
| U236/U | 4.989E−03 | 5.120E−03 | −2.56 |
| Pu/FHM | 1.124E−02 | 1.132E−02 | −0.79 |
| Np/FHM | 6.245E−04 | 6.413E−04 | −2.63 |
| Pu238/Pu | 2.345E−02 | 2.081E−02 | 12.67 |
| Pu239/Pu | 5.461E−01 | 5.525E−01 | −1.16 |
| Pu240/Pu | 2.378E−01 | 2.203E−01 | 7.98 |
| Pu241/Pu | 1.381E−01 | 1.509E−01 | −8.45 |
| Pu242/Pu | 5.447E−02 | 5.551E−02 | −1.87 |
| Am241/FHM | 4.967E−05 | 4.877E−05 | 1.85 |
| Am243/FHM | 1.439E−04 | 1.546E−04 | −6.91 |

No standard deviation is reported for the OECD simulations because only one research group reported isotopic concentrations.

Table 4
Phase 4A Benchmark $k_{inf}$ compared to those obtained with our model

| Case: Pu-vector/burnup | OECD | This model | $\sigma$ | Diff |
|---|---|---|---|---|
| 1: A/0 | 1.3021 | 1.3002 | 0.0045 | 0.0019 |
| 10: A/60 | 1.1810 | 1.1809 | 0.0043 | 0.0001 |
| 20: B/0 | 1.4065 | 1.4141 | 0.0049 | −0.0076 |
| 29: B/60 | 1.1679 | 1.1714 | 0.0035 | −0.0035 |
| 39: C/0 | 1.2108 | 1.1957 | 0.0053 | 0.0151 |
| 51: C/60 | 1.1563 | 1.1459 | 0.0058 | 0.0104 |

The standard deviation for the OECD results is $\sigma$.

To date fuel cycle analyses have been hindered by their dependence on externally performed reactor physics simulations, in large part because of the computation time and complexity involved in the latter. This is especially true for time dependent fuel cycle simulations involving diverse, interacting reactor fleets. Because of its speed, ability to analyze a broad range of reactor configurations and fuel types, with good accuracy, the model we present represents a significant advance in the tools that are available for analysis of nuclear fuel cycles. As such, integration of this model into a dynamic reactor fleet analysis package is proceeding.

## References

[1] S.M. Bowman, L.C. Leal, ORIGEN-ARP: Automatic rapid process of spent fuel depletion, decay and source term analysis, DOE, Oak Ridge, TN, NUREG/CR-0200, ORNL/NUREG/CSD-2/V1/R6, Rev 6, 2000.
[2] I.C. Gauld, K.A. Litwin, Verification and validation of the ORIGEN-S code and nuclear data libraries, AECL, Chalk River, Ontario, RC-1429, COG-I-95-150, 1995.

[3] O.W. Herman, S.M. Bowman, M.C. Brady, C.V. Parks, Validation of the SCALE system for PWR spent fuel isotope composition analyses, DOE, Oak Ridge, TN, ORNL-TM/12667, 1995.
[4] M.D. Dehart, O.W. Herman, An extension of the validation of the SCALE (SAS2H) isotope predictions for the PWR spent fuel, DOE, Oak Ridge, TN, ORNL-TM/13317, 1996.
[5] A.F. Henry, Nuclear Reactor Analysis, MIT Press, Cambridge, MA, 1975.
[6] J.J. Duderstandt, L.J. Hamilton, Nuclear Reactor Analysis, Wiley, New York, NY, 1976.
[7] G.I. Bell, S. Glasstone, Nuclear Reactor Theory, Van Nostrand, New York, NY, 1970.
[8] W.M. Stacey, Nuclear Reactor Physics, Wiley, New York, NY, 2001.
[9] E.E. Lewis, G. Palmiotti, C.B. Carrico, VARIANT: VARIational anisotropic nodal transport for multidimensional Cartesian and hexagonal geometry calculation, DOE, ANL-95/40, 1995.
[10] K.L. Derstine, A code to solve one-, two-, and three-dimensional finite-difference diffusion theory problems, DOE, ANL-82-64, 1984.
[11] B.J. Toppel, The fuel cycle analysis capability REBUS-3, DOE, ANL-83-2, Rev. 2, 1990.
[12] SCALE: A modular code system for performing standardized computer analyses for licensing evaluation, NUREG/CR-2000, Rev. 6, vols. I–III, DOE, Oak Ridge, TN, ORNL/NUREG/CSD-2R6, 2000.
[13] A. Shapiro, H.C. Huria, K.W. Cho, VENTURE-PC Manual, A Multidimensional Multigroup Neutron Diffusion Code System, Version 2, University of Cincinnati, Cincinnati, OH, EGG-2582, 1990.
[14] J.F. Briesmeister, MCNP – a general Monte Carlo N-particle transport code, Version 4C, DOE, LA-13709-M, 2000.
[15] Answers for Software Service, WIMSD A Neutronics Code for Standard Lattice Physics Analysis, OECD/NEA, NEA-1507/02, 1997.
[16] M. Takano, Burnup credit criticality benchmark – result of phase 1A, NEA/NSC/DOC (93) 22, 1994.
[17] K.M. Case, F. deHoffman, G. Placzek, Introduction to the theory of neutron diffusion, DOE, Los Alamos, NM, 1953.
[18] J.R. Lamarsh, Introduction to Nuclear Reactor Theory, Addison Wesley, Reading, MA, 1972.
[19] J.R. Knight, SUPERDAN: computer programs for calculating the Dancoff factor of spheres, cylinders and slabs, DOE, Oak Ridge, TN, ORNL/NUREG/CSD/TM-2, 1978.
[20] S. Feher, J.E. Hoogenboom, P.F.A. Deleege, J. Valko, Nucl. Sci. Eng. 117 (1994) 227.
[21] J. Barratt, Theoretical and Applied Mechanics, Cornell University, Ithaca, 2003.
[22] R.E. Macfarlane, D.W. Muir, The NJOY nuclear data processing system, Version 91, DOE, Los Alamos, NM, LA-12740-M, 1994.
[23] I.I. Bondarenko, Group Constants for Nuclear Reactor Calculations, Constants Bureua, New York, NY, 1964.
[24] G.J. O'connor, Burnup criticality benchmark – Phase IV-B: results and analysis of MOX fuel depletion calculations, NEA/OECD, ISBN 92-64-02124-8, 2003.
[25] E.A. Schneider, M.R. Deinert, K.B. Cady, in: Proceedings of the Physics of Advanced Fuel Cycles, PHYSOR 2006, Vancouver, BC, 2006.
[26] J.P. Groullier, in: Proceedings of International Conference on Fast Reactors and Related Fuel Cycles, Kyoto, Japan, 1991.